

## Synthesis of Well-Defined Environmentally Responsive Polymer Brushes by Aqueous ATRP

Jayachandran N. Kizhakkedathu,<sup>†</sup> Raymond Norris-Jones,<sup>†</sup> and Donald E. Brooks<sup>\*,†,‡</sup>

Department of Pathology and Laboratory Medicine and Department of Chemistry, 2211 Wesbrook Mall, University of British Columbia, Vancouver, BC V6T 2B5, Canada

Received July 3, 2003; Revised Manuscript Received November 17, 2003

**ABSTRACT:** Functionalized anionic polystyrene latex particles with ATRP initiators were synthesized by surfactant-free shell-growth emulsion polymerization of styrene and 2-(2'-chloropropionato)ethyl acrylate (HEA-Cl). *N*-Isopropylacrylamide (NIPAM) was polymerized from these particles by surface-initiated aqueous ATRP using PMDETA/CuCl and HMTETA/CuCl catalysts to synthesize poly(*N*-isopropylacrylamide) (PNIPAM) brushes. The grafted latexes were characterized for molecular weight of the PNIPAM chains, grafting density, and hydrodynamic thickness of the grafted polymer layer. Molecular weights of the grafted PNIPAM chains depended on the monomer concentration, concentration of copper(II) complex, and the presence of external initiator in the reaction medium.  $M_n$  of the grafted chains increases with increase in the monomer concentration and decreases with addition of copper(II) complex and external initiator. The HMTETA/CuCl catalyst produces higher molecular weight chains than PMDETA/CuCl. Molecular weights from ~50 000 to 800 000 with low polydispersities, between 1.25 and 1.4, were achieved. The grafting density of PNIPAM on the surface increases with increasing monomer concentration and decreases with addition of copper(II) catalyst and external initiator. Block copolymerization of *N,N*-dimethylacrylamide from PNIPAM-grafted latex demonstrated that the chains are terminated with a chlorine atom, and the grafting reactions are taking place by the ATRP mechanism. The hydrodynamic thickness (HT) of the grafted PNIPAM layer scales as  $DP^{0.66}$  (where DP = degree of polymerization) at constant grafting density (chains/nm<sup>2</sup>). The HT values for PNIPAM brushes are sensitive to temperature and salt concentration. Since the transition from extended coil to collapsed structure occurs over a range of temperature and salt concentration, it follows a second-order transition, as predicted by theory. The thickness of the collapsed brush is sensitive to the type of stimulus used to induce the phase transition.

### Introduction

Controlled syntheses of stimulus-sensitive surfaces are challenging but have potential applications in biotechnology and the biomedical field.<sup>1,2</sup> Such surfaces can be synthesized by different methods such as deposition of monolayers, plasma modification, adsorption of synthetic polymers or natural macromolecules, and formation of polymer brushes.<sup>1,3–6</sup> Polymer surface layers exhibiting a change in dimensions and properties with environmental variations such as pH, salt concentration, or temperature could have applications in many fields such as chromatography, responsive membranes, protein adsorption, and cell attachment.<sup>7–14</sup>

Over the past decade, several methods have been developed for the controlled synthesis of tethered polymers from surfaces.<sup>15</sup> When polymer chains are grafted by one end to the surface at such a high density that the average distance between the chains is lower than twice the radius of gyration of the free polymer chain, the grafts are referred to as polymer brushes.<sup>15,16</sup> The “grafting from” method, in which polymerization is initiated on the surface, has been used extensively for the controlled synthesis of high-density polymer brushes. Using this approach, several controlled/living polymerization techniques such as anionic,<sup>17</sup> cationic,<sup>18</sup> and atom transfer radical polymerization (ATRP)<sup>19–23</sup> have been used to synthesize polymer brushes from ap-

propriately functionalized surfaces with high efficiency. One other advantage is that the polymer chains grown by these methods can be reinitiated by the addition of fresh monomer and catalyst to form block copolymer brushes.<sup>24</sup>

Among the methods reported, ATRP is the most versatile due to its tolerance to a variety of reaction conditions and monomers.<sup>19–21,23,25</sup> Aqueous ATRP has been used to synthesize several hydrophilic polymers in solution or on surfaces of biomedical interest.<sup>23,25,26–30</sup> Extremely thick polymer layers and high molecular weight polymer chains have been achieved on surfaces by this method.<sup>23,28</sup> Although it is difficult to polymerize substituted acrylamides by ATRP in organic media,<sup>31–33</sup> we have had considerable success growing poly(*N,N*-dimethylacrylamide) grafts with controlled chain density and molecular weights from surfaces in aqueous media.<sup>23,29,30</sup>

Poly(*N*-isopropylacrylamide) (PNIPAM) is a water-soluble polymer that exhibits a lower critical solution temperature (LCST) around 32 °C in aqueous solution.<sup>34</sup> It assumes a random coil structure below the LCST but forms a more collapsed globular structure above this temperature.<sup>34–36</sup> This polymer also undergoes a coil globule phase transition with the addition of salts or other hydrogen bond breaking agents in water.<sup>36</sup> The collapsed state has more hydrophobic character than the more extended coil.<sup>2,37</sup> Because of this unusual property, PNIPAM has been widely used in synthesizing stimuli responsive materials.<sup>38–40</sup>

In the case of surfaces grafted with PNIPAM, one could take the advantage of the coil–globule transition

<sup>†</sup> Department of Pathology and Laboratory Medicine.

<sup>‡</sup> Department of Chemistry.

\* To whom correspondence should be addressed: phone (604) 822-7081, Fax (604) 822-7635; e-mail don.brooks@ubc.ca.

to control the structure and properties of the grafted layer and thus the properties of the surface itself.<sup>2,37,38</sup> Although there are some reports on PNIPAM layers on different surfaces,<sup>7,8,41</sup> parameters such as the density of chains on the surface, molecular weight, and polydispersity of chains are rarely available. Such information is required to interpret system behavior since these properties need to be controlled if reproducible manipulation of, for instance, wettability, cell adhesion, or macromolecular adsorption is to be achieved.

In this paper we report for the first time the controlled synthesis of PNIPAM brushes by aqueous ATRP at room temperature. PNIPAM was grown from negatively charged polystyrene latex surfaces functionalized with ATRP initiators to achieve high molecular weights and narrow polydispersities. Grafted polymer chains were characterized for their molecular weight, polydispersity, and grafting density on the surface. We also demonstrated the reinitiation of the surface PNIPAM chains by an efficient block copolymerization method. The hydrodynamic thickness of the grafted PNIPAM layers was sensitive to temperature and various environmental conditions.

## Experimental Section

Styrene (Aldrich, 99%) was first washed with a 1% NaOH solution, dried, and then distilled under reduced pressure. *N*-Isopropylacrylamide (NIPAM; Aldrich, 97%) was purified by crystallization from hexane and stored at  $-20^{\circ}\text{C}$  until used. *N,N*-Dimethylacrylamide (DMA; Aldrich, 99%) was distilled in a vacuum and stored under argon at  $-80^{\circ}\text{C}$ . *N,N,N',N',N'*-Pentamethyldiethylenetriamine (PMDETA; Aldrich, 99%), 1,1,4,7,10,10-hexamethyltriethylenetetramine (HMTETA; Aldrich, 97%), CuCl (Aldrich, 99+%), and CuCl<sub>2</sub> (Aldrich, 99.99%) were used as received. All other commercial reagents were purchased of highest purity from Aldrich and used without further purification. 2-(2'-Chloropropionato)ethyl acrylate (HEA-Cl) was synthesized as described in our earlier report.<sup>23</sup> Water purified using a Milli-Q Plus water purification system (Millipore Corp., Bedford, MA) was used in all experiments.

Nuclear magnetic resonance was performed on a Bruker Avance 300 NMR spectrometer using deuterated solvents (CDCl<sub>3</sub>, Cambridge Isotope Laboratories, 99.8% D) with the solvent peak as a reference. Reverse phase HPLC analyses for monomer conversion measurements were done on a Hitachi model L-6210 HPLC fitted with a L-4200 UV-vis detector and a LiChrospher 60 RP-select B (10  $\mu\text{m}$ ) silica-based reverse phase column (5  $\times$  1 cm) from Merck, with detection at  $\lambda = 236\text{ nm}$  using aqueous 0.1% trifluoroacetic acid (TFA) solution as the mobile phase at a flow rate of 4 mL/min at  $22^{\circ}\text{C}$ .

Molecular weights were determined by gel permeation chromatography (GPC) on a Waters 2690 separation module fitted with a DAWN EOS multiangle laser light scattering (MALLS) detector from Wyatt Technology Corp. with 18 detectors placed at different angles (laser wavelength  $\lambda = 690\text{ nm}$ ) and a refractive index detector from Viscotek Corp. operated at  $\lambda = 620\text{ nm}$ . Aqueous 0.1 N NaNO<sub>3</sub> solution was used as the mobile phase at a flow rate of 0.8 mL/min. Aliquots of 200  $\mu\text{L}$  of the polymer solution were injected through two Waters Ultrahydrogel columns at  $22^{\circ}\text{C}$  (guard column, Ultrahydrogel linear with bead size 6–13  $\mu\text{m}$ , elution range  $10^3$ – $7 \times 10^6\text{ Da}$  and Ultrahydrogel 120 with bead size 6  $\mu\text{m}$ , elution range  $150$ – $5 \times 10^3\text{ Da}$ ) connected in series. The value of  $dn/dc$  for PNIPAM in the mobile phase at  $22^{\circ}\text{C}$  was determined at  $\lambda = 620\text{ nm}$  to be 0.164 mL/g and was used for determining molecular weight parameters.

Particle size measurements (i.e., measurements of the hydrodynamic diameter distribution of particle suspensions) were carried out on a temperature-controlled Beckman Coulter N4 Plus particle size analyzer with an analysis range of 3–3000 nm. Aqueous dispersions of particles were allowed to

thermally equilibrate for 5 min, and the measurements were made at  $20^{\circ}\text{C}$  at an angle of  $90^{\circ}$  unless otherwise noted. Size analyses were performed using the software supplied by the manufacturer. Conductometric titrations were done on YSI model 35 conductance meter and 3403 cell with platinum electrode at  $25^{\circ}\text{C}$ . A syringe pump (Harvard Instruments) was used to inject dilute NaOH at a constant flow rate of 0.0102 mL/min.

A narrowly dispersed batch of polystyrene seed latex (PS seed latex) was synthesized by surfactant-free emulsion polymerization of styrene and characterized by reported procedures.<sup>23</sup> The average hydrodynamic size of the latex particles was 509 nm measured by the particle size analyzer.

**Shell Growth Polymerization: Synthesis of the ATRP Initiator Layer.** An aqueous suspension of PS seed latex particles (3.33 wt %, 523 g) was heated to  $70^{\circ}\text{C}$  with stirring at 350 rpm, degassed, and purged with argon. Styrene (5.21 g, 0.05 mol) and HEA-Cl (3.5 g, 0.017 mol) were added successively to the suspension 10 min apart, and shell polymerization was initiated with potassium persulfate (KPS) (0.200 g, 0.74 mmol in 30 mL of water, degassed) 5 min later. The reaction was continued for 6 h. The latex was then cleaned by dialysis against water for 1 week with frequent changes followed by five cycles of centrifugation and resuspension. The solid content was determined by freeze-drying. The shell latex was characterized as described in the analysis section.

**Aqueous Atom Transfer Radical Polymerization from Latex. General Method for Grafting of NIPAM.** All reactions were performed in a glovebox filled with argon due to the sensitivity of the Cu(I) complex to air. A suspension of latex (22 g, 3 wt %) carrying the ATRP initiator layer was degassed for 2.5 h by continuous vacuum and argon cycles and transferred to the glovebox. Brij-35 (nonionic surfactant) (0.035 g, 0.16 wt %) was added to the suspension and stirred for 5 min. For a typical reaction, NIPAM (0.20 g, 1.7 mmol) was stirred with HMTETA (8.6 mg, 37  $\mu\text{mol}$ ), CuCl (1.5 mg, 15  $\mu\text{mol}$ ), CuCl<sub>2</sub> (0.4 mg, 3.0  $\mu\text{mol}$ ), and Cu powder (1.0 mg, 16  $\mu\text{mol}$ ) for 3 min; 3.5 g (3% w/w) of degassed Brij-35 stabilized PS shell latex (PSL) was added to this under stirring at room temperature ( $22^{\circ}\text{C}$ ). The reaction was continued for 24 h, and monomer conversion was determined by analyzing the supernatant solution by reverse phase HPLC. The grafted latex was cleaned by repeated sequential centrifugation and resuspension in water, NaHSO<sub>3</sub> solution (50 mM), and water to remove adsorbed copper complexes for 8–10 cycles until there was no detectable amount of polymer, monomer, or catalyst in the supernatant.

Different sets of experiments were conducted by changing the catalyst, monomer concentration, and CuCl<sub>2</sub> concentration and with addition of external initiator. The same concentrations of catalyst and latex were used for all grafting reactions unless otherwise mentioned.

**Block Copolymerization.** Latex particles grafted with PNIPAM chains were synthesized by following the general method for aqueous ATRP. HMTETA (54.0 mg, 0.23 mmol), CuCl (4.6 mg, 46  $\mu\text{mol}$ ), CuCl<sub>2</sub> (12.0 mg, 88  $\mu\text{mol}$ ), Cu powder (4 mg, 63  $\mu\text{mol}$ ), NIPAM (0.88 g, 7.7 mmol), methyl 2-chloropropionate (2  $\mu\text{L}$ ), and 15 g of 3.0 wt % degassed PSL stabilized with Brij-35 (0.024 g) were used for this reaction. Reaction conditions were the same as in the previous section.

A second block of PDMA was added to the first PNIPAM by a copolymerization reaction of DMA with the PNIPAM grafted latex. PNIPAM grafted latex (1.75 wt %, 3 g), HMTETA (14.4 mg, 62  $\mu\text{mol}$ ), CuCl (1.3 mg, 13  $\mu\text{mol}$ ), CuCl<sub>2</sub> (3.0 mg, 22  $\mu\text{mol}$ ), Cu powder (1 mg, 16  $\mu\text{mol}$ ), and DMA (0.5 g, 5 mmol) were used. The PNIPAM grafted latex was degassed and added to the solution of catalyst and monomer in a glovebox. The reaction was stopped after 48 h, and the grafted latex particles were cleaned and analyzed. Both PNIPAM and PNIPAM-*b*-PDMA grafted latex particles were characterized for molecular weight and hydrodynamic thickness of the grafted layer.

**Analysis of the Shell and Polymer Grafted Latex.** Shell latex was analyzed for hydrodynamic size, surface initiator concentration, and surface charge density. The hydrodynamic size of the latex was determined by particle size analysis. The

accessible surface initiator concentration was calculated from a conductometric titration of saponified latex as reported earlier.<sup>23,42,43</sup> For a typical case PSL (2 g) was stirred with 1 mL of 2 N NaOH for 36 h at room temperature. The suspension was centrifuged and washed several times with water to remove excess of NaOH present in the medium. The pellet was resuspended in Milli-Q water and acidified with 0.1 N HCl. The centrifugation and washing continued until the pH of the supernatant reached  $\sim 7.0$ . Conductometric titration with 0.02 N NaOH (standardized using potassium hydrogen phthalate) gave the total negative charge on the surface which was the sum of the sulfate surface charge and the carboxyl groups produced from hydrolysis of the initiator.<sup>23,42,43</sup> Latex surface charge was determined from conductometric titration of unhydrolyzed latex carried out by washing with diluted HCl and then water to neutrality followed by titration with NaOH; the difference between the two values gave the surface concentration of the initiator. The total concentration of HEA-Cl incorporated into the latex was determined from  $^1\text{H}$  NMR spectra of freeze-dried samples dissolved in  $\text{CDCl}_3$ . From the ratio of the intensities of peaks at 4.1–4.3 ppm ( $-\text{O}-\text{CH}_2-\text{CH}_2-\text{O}-$  and  $-\text{CHCl}-$ ) and peaks of aromatic protons from polystyrene (6.7–7.2 ppm) the mole percent of HEA-Cl present in the latex was calculated.

The grafted latex was characterized by hydrodynamic size measurements utilizing the particle size analyzer and by analysis of the polymer released by hydrolysis. We define the difference between the grafted and shell latex radii to be the hydrodynamic thickness (HT) of the grafted layer at 20 °C. Characterization of the polymer chains (molecular weight, molecular weight distribution, mass of the grafted chains per unit area of latex, and radius of gyration,  $R_g$ ) grown from the surface was performed by quantitative cleavage of the chains and analysis by GPC-MALLS. A known amount of grafted latex (2 g) was stirred with 0.5 mL of 2 N NaOH (final concentration  $\sim 0.35$  N) at 4 °C until no change in the amount released was detected (3 weeks). The supernatant and washings were collected and analyzed by GPC. The mass of polymer in solution following cleavage was determined using a calibrated RI detector.

**Sensitivity of Grafted Polymer Brushes to Temperature and Salt Concentration.** The hydrodynamic sizes of grafted particles in aqueous dispersions were monitored under different conditions using the temperature-controlled particle size analyzer. In one set of experiments, the temperature of the medium was changed from 18 to 40 °C with an increment of 2 °C at pH 7.1. An equilibration time of 15 min was allowed at each temperature before three consecutive measurements of hydrodynamic size were taken, the average of which is reported. The hydrodynamic size of the particles was also monitored in this way through a cooling cycle; the data collected during a single continuous heating and cooling cycle are reported.

In another set of experiments the hydrodynamic size was measured as a function of NaCl and  $\text{Na}_2\text{SO}_4$  concentration. A set of solutions with different salt concentrations was made and the pH adjusted to 7.4 with 0.5 M sodium bicarbonate solution. The latex suspension was added to the solutions and equilibrated for 5 min, and the hydrodynamic size of the particles at 20 °C was determined as the average value of three consecutive measurements.

## Results and Discussion

Polystyrene latex provides a good model surface for the study of properties and mechanisms of surface-initiated ATRP in aqueous solutions. Because of the large specific surface area, there is sufficient grafted polymer available for unambiguous analysis following cleavage from the surface. Another advantage of latex is that surface properties can be changed readily. One can design surfaces having different amounts of initiators, different charges, and varying charge densities by changing reaction conditions for the latex synthesis.<sup>23,30,44</sup>

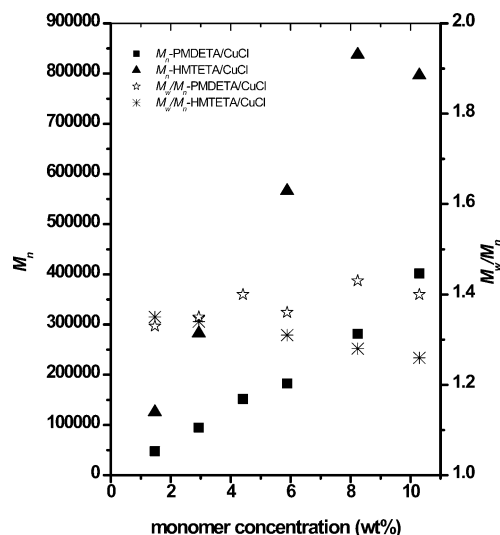


**Figure 1.** Dependence of  $M_n$  and  $M_w/M_n$  of grafted PNIPAM with monomer concentration for PMDETA/CuCl and HMTETA/CuCl measured by GPC-MALLS. Experimental conditions: 3.5 g of 3 wt % suspension of latex,  $N,N,N,N,N'$ -pentamethyldiethylenetriamine (PMDETA 40  $\mu\text{mol}$ ) or 1,1,4,7,10,10-hexamethyltriethylenetetramine (HMTETA 37  $\mu\text{mol}$ ) CuCl (15  $\mu\text{mol}$ ),  $\text{CuCl}_2$  (3.0  $\mu\text{mol}$ ), copper powder (16  $\mu\text{mol}$ ) at 22 °C. Surface initiator concentration =  $(1.56 \pm 0.05) \times 10^{-6}$  mol/ $\text{m}^2$ .

We have shown in earlier reports that aqueous ATRP of hydrophilic monomers from a latex surface is very different from ATRP in solution or from surfaces carried out in low dielectric constant media. Because the catalyst is positively charged and the surface is negatively charged in most cases, the surface region is enriched with catalyst due to electrostatic interactions,<sup>23,44</sup> which has a strong effect on polymerization and graft properties. Proper consideration of these factors leads to well-controlled grafts of unprecedented surface concentration, molecular weight, and thickness.<sup>23,29</sup>

In this work we have synthesized and characterized anionic latex particles functionalized with ATRP initiators by following our reported procedure.<sup>23</sup> The surface initiator concentration of the latex particles, obtained from conductometric titration following saponification, was  $(1.54 \pm 0.05) \times 10^{-5}$  mol/g or  $(1.56 \pm 0.05) \times 10^{-6}$  mol/ $\text{m}^2$ . This compares to a total HEA-Cl concentration of  $7.15 \times 10^{-4}$  mol/g determined by  $^1\text{H}$  NMR, implying that only 2.15% of the initiator is accessible from aqueous solution. The charge density on the surface, due to sulfate groups from the KPS shell initiator was  $(4.7 \pm 0.1) \times 10^{-7}$  mol/ $\text{m}^2$  or  $0.046 \pm 0.001$  C/ $\text{m}^2$ . The average diameter of the latex particles determined by the particle size analysis was 584 nm with narrow polydispersity. The shell thickness upon addition of ATRP initiator layer of the PSL is 37 nm calculated from the increase in the diameter of the shell latex compared to seed PS latex. A series of experiments were carried out to understand the effect of monomer concentration, concentration of Cu(II), and soluble external initiator on the surface-initiated polymerization of NIPAM.

**Effect of Monomer Concentration.** Figure 1 shows the dependence on monomer concentration of molecular weight ( $M_n$ ) and polydispersity ( $M_w/M_n = \text{PDI}$ ) of PNIPAM grafted onto the functionalized polystyrene latex catalyzed by two different ligand/copper chloride combinations, PMDETA/CuCl and HMTETA/CuCl. With increasing monomer concentration from 1.5 to 10.30 wt



**Table 1. Effect of Monomer Concentration on Conversion, Distance between the Grafted Chains (*D*), Grafting Density (chains/m<sup>2</sup>), *D*/*R*<sub>g</sub>, and Hydrodynamic Thickness (HT) of Aqueous ATRP of NIPAM on Functionalized Latex Particles**

sample code	monomer concn (wt %)	conv (wt %)	<i>D</i> (nm)	<i>D</i> / <i>R</i> <sub>g</sub> <sup>a</sup>	grafting density (chains/m <sup>2</sup> ) × 10 <sup>-16</sup>	HT (nm)
1 <sup>b</sup>	1.5	42	5.3	0.665	3.62	102
2 <sup>b</sup>	2.9	55	4.1	0.317	6.07	131
3 <sup>b</sup>	4.4	61	3.7	0.220	7.14	228
4 <sup>b</sup>	5.9	62	3.6	0.189	7.93	221
5 <sup>b</sup>	8.2	65	4.1	0.171	6.06	390
6 <sup>b</sup>	10.3	63	4.0	0.136	6.31	603
7 <sup>c</sup>	1.5	ND	5.6	0.384	3.13	132
8 <sup>c</sup>	2.9	ND	4.8	0.203	4.26	405
9 <sup>c</sup>	4.4	ND	3.6	0.118	7.86	380
10 <sup>c</sup>	5.9	ND	4.5	0.123	4.91	483
11 <sup>c</sup>	8.2	ND	6.0	0.134	2.73	585
12 <sup>c</sup>	10.3	ND	5.0	0.104	4.35	582

<sup>a</sup> *R*<sub>g</sub> = radius of gyration (nm) measured by MALLS. <sup>b</sup> Experiments with PMDETA/CuCl. <sup>c</sup> Experiments with HMTETA/CuCl; ND = not determined. Experimental conditions: 3.5 g of 3 wt % suspension of latex: Cu(I) complex (15 μmol), Cu(II) complex (3 μmol), Cu powder (16 μmol), reaction temperature 22 °C. Surface initiator concentration =  $(1.56 \pm 0.05) \times 10^{-6}$  mol/m<sup>2</sup> of latex.

% the *M*<sub>n</sub> of the grafted polymer increases for both catalysts. The molecular weight of the grafted polymer increases from ~50 000 to 800 000 with monomer concentration. HMTETA/CuCl produces a higher molecular weight than PMDETA/CuCl under identical reaction conditions. The PMDETA/CuCl catalyst produces polymers with polydispersities around 1.4 for all the monomer concentrations studied. Since the uncertainty in PDI calculated by ASTRA software is ±0.05, we feel no regular trend was demonstrated. With HMTETA/CuCl the PDI decreases from 1.35 to 1.25 with increasing monomer concentration and so may be significant. Considering the high molecular weight of the polymers, the standard deviation in the calculation of PDI, and the fact that the data resulted from six independent experiments, a large number of reactions would have to be done to prove the point. The difference in reactivity of PMDETA/CuCl compared to that of HMTETA/CuCl may be the reason for the lower molecular weight of the grafted polymers produced in the former system. It has been reported that tetradentate HMTETA produces more reactive complexes than PMDETA complexes in other ATRP reactions.<sup>45</sup> An additional reason for the lower molecular weight of PNIPAM produced by PMDETA/CuCl may be the higher grafting density of chains in this system (Table 1).

In all the polymerization reactions the latex suspensions became viscous with time, particularly as the monomer concentration was increased. The viscosity increase was more evident with HMTETA/CuCl than with PMDETA/CuCl used under identical conditions, so much so that it was difficult to stir the reaction medium at high monomer concentration when using HMTETA/CuCl. The small decrease in graft molecular weight with HMTETA/CuCl at 10.3 wt % monomer concentration (Figure 1) may be due to the hindered diffusion of monomer and catalyst in these viscous suspensions.

The number of chains grafted per unit area and average distance between the polymer chains (assuming a square lattice) for the two catalyst combinations are given in Table 1. The grafting density tends to increase with monomer concentration for both catalysts, but the

effect is more pronounced at low monomer concentrations for both the catalysts and the grafting density becomes independent of monomer concentration at high monomer concentrations. We have argued elsewhere,<sup>23,29</sup> and below, that this may be due to an insufficient rate of monomer diffusion to the initiation surface relative to the initiation rate at low monomer concentration that does not occur at higher monomer levels.

PMDETA/CuCl generally gives higher grafting densities than HMTETA/CuCl, showing that more chains are initiated for this catalyst under identical reaction conditions. The results are similar to DMA,<sup>23</sup> but the grafting density here is less dependent on monomer concentration. Since we are using the same shell latex for these reactions, a difference in accumulation of the two positively charged catalysts on the surface could be responsible for the observation. We reported earlier that under similar conditions PMDETA/CuCl accumulates more on the latex surface than HMTETA/CuCl<sup>23</sup> and that it also produces higher chain densities with DMA, consistent with the present results.

Another factor affecting polymerization is the concentration of monomer near the surface. The present results show that NIPAM produces a lower grafting density than DMA under identical conditions. This suggests that, as well as catalyst concentration, monomer type also influences grafting chemistry. The accessibility and diffusion of monomer near the interface depend on the chemical nature of the monomer and the surface. Thus, a monomer with affinity for a particular surface could concentrate there and influence the early stages of polymerization.<sup>23</sup> It is not clear whether monomer-surface affinity would enhance or inhibit polymerization, however, as monomer binding could act to reduce its availability to the reactive oligomer ends or could provide a source of monomer to enhance polymerization, depending on the adsorption off rate relative to the on rate and propagation rate. We have no direct information on the surface concentration of either DMA or NIPAM; attempts to determine the adsorption of monomers by its depletion from the supernatant using an HPLC method provided equivocal results (Supporting Information). However, we can infer some relevant information by examining the amount of solution polymerization compared to the amounts grafted.

We have shown earlier that in the case of DMA some solution polymerization occurs simultaneously with graft polymerization that decreases in relative amount with increases in the monomer concentration in the medium. Solution polymerization occurs due to a radical transfer reaction occurring at an early stage of polymerization. It seems likely that this is due to a local monomer deficiency near the site of surface polymerization, allowing the free radical to transfer to solvent or ligand.<sup>23</sup> From our results, it is clear that the NIPAM produces more solution polymer than DMA (Table 2; cf. Table 3 (ref 23) or Table 6 (ref 29)). This suggests that NIPAM is less available near the surface reaction sites than DMA, perhaps because it is a more hydrophobic monomer and could adsorb to the exposed polystyrene surface. We observed similar solution polymerization in conjunction with surface grafting reactions for a number of monomers we have studied, e.g., methoxyethylacrylamide, hydroxyethyl acrylate, and PEG acrylamides (unpublished results).

One other factor involved may be polymer adsorption to the latex early in the polymerization reaction. It is

**Table 2.** Comparison of Solution Polymer vs Graft Polymer

sample code	solution polymer		graft polymer		% soln <sup>a</sup>	% graft <sup>a</sup>
	$M_w$	$M_w/M_n$	$M_w$	$M_w/M_n$		
1 <sup>b</sup>	67 000	1.33	63 000	1.33	86.2	13.8
2 <sup>b</sup>	117 800	1.42	128 000	1.35	82.4	17.6
3 <sup>b</sup>	183 000	1.50	212 000	1.4	80.0	20.0
4 <sup>b</sup>	240 000	1.55	248 000	1.36	80.3	19.7
5 <sup>b</sup>	430 050	1.61	402 000	1.43	84.1	15.9
6 <sup>b</sup>	547 800	1.80	562 000	1.4	80.1	19.6
8 <sup>c</sup>	483 000	1.72	379 000	1.34	ND <sup>d</sup>	ND <sup>d</sup>
9 <sup>c</sup>	520 000	1.85	292 000	1.33	ND <sup>d</sup>	ND <sup>d</sup>
10 <sup>c</sup>	743 000	1.93	742 000	1.31	ND <sup>d</sup>	ND <sup>d</sup>
11 <sup>c</sup>	1 141 000	1.53	1 072 000	1.28	ND <sup>d</sup>	ND <sup>d</sup>
12 <sup>c</sup>	1 292 000	1.39	1 004 000	1.26	ND <sup>d</sup>	ND <sup>d</sup>

<sup>a</sup> Calculated from difference in total the amount of polymer formed (from monomer conversion by HPLC analysis) and amount grafted from GPC analysis. <sup>b</sup> Experiments with PDMETA/CuCl. <sup>c</sup> Experiments with HMTETA/CuCl. Experimental conditions: 3.5 g of 3 wt % suspension of latex: Cu(I) complex (15 mmol), Cu(II) complex (3 mmol), Cu powder (16 mmol), reaction temperature 22 °C. Surface initiator concentration =  $(1.56 \pm 0.05) \times 10^{-6}$  mol/m<sup>2</sup> of latex. <sup>d</sup> ND = not determined.

known that PNIPAM adsorb to PS latex from solution<sup>35,46</sup> and the adsorption of PNIPAM is higher than PDMA. The adsorbed PNIPAM could inhibit diffusion of monomer to reaction sites near the surface during polymerization.

The grafting density values presented in this paper may be slightly in error due to PNIPAM adsorption to the latex surface during the cleavage process. We think it is minimal, however, as measured values for adsorbed PNIPAM on latex are <1% of the amounts released following saponification<sup>35,46</sup> (Tables 1 and 2).

The total conversion of NIPAM monomer with varying monomer concentration is given Table 1. Monomer conversion increased with increasing monomer concentration. We could not measure the monomer conversion for reactions catalyzed by HMTETA/CuCl as the reaction medium was too viscous. The difference between the amount of monomer polymerized and the grafted amount gives the mass of polymer in solution. Over 80% of the polymers formed were found in solution, but the solution product has essentially identical molecular weight characteristics to the grafted material.

Initial activation of the free radical and the subsequent first few monomer additions are critical for surface initiated polymerization,<sup>23</sup> since once the growing end is removed from the influence of the surface it would be expected to react much as in any solution polymerization. We have suggested earlier that there is a greater chance of radical transfer to the tertiary amine complex (catalyst) or solvent at this early stage of chain growth.<sup>23</sup> The positively charged catalyst used in our reactions accumulates near the negatively charged latex surface due to electrostatic interactions. This could increase the chance of chain transfer to the catalyst as tertiary amines are known to be good radical chain transfer agents.<sup>47</sup> This is consistent with our observation that latex particles with a larger negative charge density give lower grafting densities and more solution polymerization.<sup>44</sup> The monomer-starved conditions at the surface also facilitate radical transfer at early stages of the reaction.

Early transfer of radicals is also suggested by the identical molecular weights of the grafted and solution polymers (Table 2). This suggests that significant chain

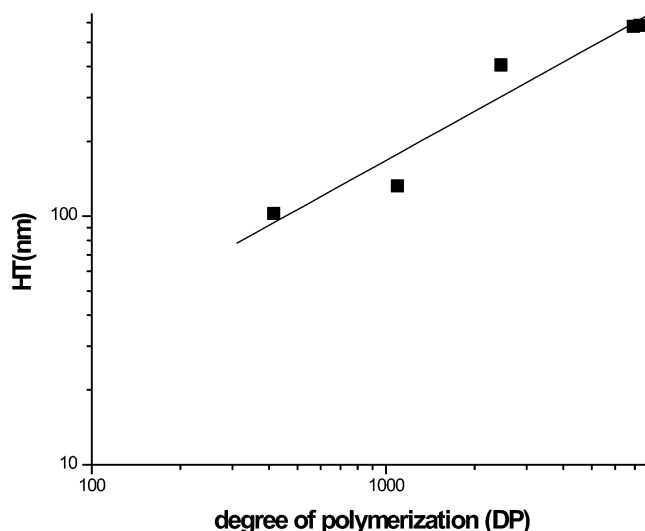


**Figure 2.** Dependence of hydrodynamic thickness of PNIPAM brushes on degree of polymerization (DP) at constant grafting density of  $0.036 \pm 0.007$  chains/nm<sup>2</sup>. A linear fit method was used to evaluate the exponent to DP from the equation  $HT \propto (DP)^{a(\sigma)^b}$  (ref 45 in the main text). The HT values are measured by a temperature-controlled particle size analyzer at 20 °C and are given in Table 1.

transfer does not occur during the polymer growth stage, an argument that is supported by the low polydispersity of the grafts and highly efficient block copolymerization, which will be discussed in the next section.

We know from past experiments that the nature of the surface, surface initiator density, surface charge density, the nature of the catalyst and monomer concentration all influence surface-initiated aqueous ATRP reactions.<sup>23,29,30,44</sup> The results presented here show that an additional factor, the nature of the monomer, also influences polymerization from surfaces. Our results indicate that for successful surface-initiated polymerization a unique set of reaction conditions is required for a particular monomer/catalyst pair.

$D/R_g$  values and hydrodynamic thickness (HT) values for the synthesized polymer brushes are given in Table 1, where  $D$  is the average distance between the grafted chains and  $R_g$  is the radius of gyration of the polymer in solution, measured by MALLS. The small values of  $D/R_g$  indicate that all the grafted layers are in the brush regime ( $D/R_g < 2$ ) and are highly strained. The large hydrodynamic thickness values for the polymer layer support this argument (Table 1). The hydrodynamic thickness of the brush is always greater than the unperturbed dimension of the polymer in solution. The HT increases with increasing monomer concentration of the initial reaction mixture and molecular weight of the grafted polymer, as expected.

The dependence of HT on the degree of polymerization (DP) at constant grafting density ( $0.036 \pm 0.007$  chains/nm<sup>2</sup>) is given in Figure 2. The least-squares slope of the log-log curve is  $0.66 \pm 0.10$ , implying that HT varies as  $(DP)^{0.66}$ . This demonstrates that HT values for these PNIPAM brushes are smaller than for the corresponding planar brushes of equal DP and  $\sigma$ , since for planar brushes the scaling is  $HT \sim (DP)^{1.0}$  at constant grafting density.<sup>49,50</sup> The reason is that brushes on spherical surfaces have a larger volume in which into which they can expand at greater radial positions, reducing brush thickness. The exponent for DP indicates that the brushes in the present study behave as being intermediate between true spherical and planar systems.<sup>48</sup>

**Table 3. Comparison of Grafting Density ( $\sigma$ , chains/nm<sup>2</sup>) of PNIPAM Brushes with Height of the Brush**

sample code	$\sigma$ at the latex surface (chains/nm <sup>2</sup> ) <sup>a</sup>	$\sigma$ at the outer edge of brush (chains/nm <sup>2</sup> ) <sup>b</sup>	ratio <sup>c</sup>	sample code	$\sigma$ at the latex surface (chains/nm <sup>2</sup> ) <sup>a</sup>	$\sigma$ at the outer edge of brush (chains/nm <sup>2</sup> ) <sup>b</sup>	ratio <sup>c</sup>
1	0.036	0.0198	1.8	7	0.031	0.0148	2.1
2	0.061	0.0288	2.1	8	0.043	0.0074	5.7
3	0.071	0.0224	3.2	9	0.078	0.0148	5.2
4	0.079	0.0257	3.1	10	0.049	0.0069	7.0
5	0.060	0.0110	5.5	11	0.027	0.0030	9.0
6	0.063	0.0067	9.4	12	0.043	0.0049	8.9

<sup>a</sup> Original grafting density at the surface of latex particles calculated from the surface area of the latex particles and amount of PNIPAM grafted. <sup>b</sup> Apparent graft density at the outer edge of the brush calculated from the apparent increase in the surface area of the particles on grafting PNIPAM chains. <sup>c</sup> Ratio of  $\sigma$  at the surface and outer edge.

PNIPAM brushes have a greater hydrodynamic thickness than PDMA brushes of the same molecular weight and chain density.<sup>23</sup> This suggests that the nature of the pendent groups on the polymer plays a role in the extension of chains from the surface in a confined state. We are currently investigating the effect of different pendent groups on brush height as a function of grafting density and molecular weights which will be published at a later date.

It has been calculated from theoretical models that the chain concentration in the brush layer for a spherical brush monotonically decreases with distance from the surface, in a way that differs from planar brushes.<sup>51</sup> The magnitude of the effect can be illustrated by calculating the apparent chain density at the edge of the brush, as defined by HT (Table 3). This gives a qualitative idea of the chain concentrations in the brush layer, the density decreasing, for instance, from 0.043 chains/nm<sup>2</sup> at the latex surface to 0.0049 chains/nm<sup>2</sup> at the edge of the brush layer. Though the interchain separation at the outer edge of the polymer brush increases with increases in HT, the grafted chains are still in the brush regime in all cases illustrated, i.e., they obey  $(\sigma_{\text{app}}^{-1/2}/R_g) < 2$ , meaning that the chain separation at the end of the brush layer is much smaller than the  $2R_g$  values of the grafted polymer in solution. The strain experienced by chains in the direction normal to surface decreases with increase in the brush height due to the increased volume available as the radial position increases. This effect reduces the brush height for spherical brushes whose thickness is significant relative to the particle radius, relative to planar brushes of the same molecular weight and grafting density.<sup>48,51</sup>

**Effect of CuCl<sub>2</sub> and External Initiator Concentration.** It has been reported that Cu(II) complexes are deactivators in ATRP reactions.<sup>19,21,52</sup> We showed earlier that the addition of Cu(II) complexes improves the PDI and decreases the molecular weight of grafted PDMA chains in aqueous ATRP grafting reactions.<sup>23</sup> Here we examined the effect of an increased concentration of Cu(II) complex with respect to Cu(I) complex on the polymerization of NIPAM from surfaces. The reaction conditions were similar to those of previous experiments except for the addition of a higher amount of Cu(II) complex at the beginning of the reaction. The monomer conversion, molecular weight, and PDI of the grafted polymer and grafting density are given in Table 4. Total monomer conversion and molecular weight of the grafted chains decrease with increase in Cu(II) complex concentration. The addition of extra Cu(II) complex decreases the propagation rate by increasing the deactivation of free radicals in the system and shifting the ATRP equilibrium more toward the dormant species.

The PDI of the grafted PNIPAM increases slightly and the grafting density decreases with increasing

**Table 4. Effect of CuCl<sub>2</sub> and External Initiator on the  $M_n$  and Other Properties of PNIPAM Brushes<sup>a</sup>**

Cu(II) <sup>b</sup>	external initiator ( $\mu\text{L}$ )	$M_n$	$M_w/M_n$	$D^c$ (nm)	$R_g^d$ (nm)	HT <sup>e</sup> (nm)
20	0	566 000	1.31	4.5	36.7	483
100	0	290 000	1.38	6.4	25.3	316
200	0	133 000	1.46	7.0	14.8	245
200	0.5	126 000	1.22	8.1	14.4	153
200	1.0	102 000	1.20	6.3	12.8	143

<sup>a</sup> Monomer concentration 5.88 wt %, HMTETA/CuCl catalyst, and methyl 2-chloropropionate as external initiator were used. <sup>b</sup> mol % of Cu(II)Cl<sub>2</sub> relative to Cu(I)Cl. <sup>c</sup> Distance between the grafting sites. <sup>d</sup> Radius of gyration measured by GPC-MALLS. <sup>e</sup> Hydrodynamic thickness. Experimental conditions: 3.5 g of 3 wt % suspension of latex: Cu(I) complex (15  $\mu\text{mol}$ ), Cu powder (16  $\mu\text{mol}$ ), reaction temperature 22 °C. Surface initiator concentration =  $(1.56 \pm 0.05) \times 10^{-6}$  mol/m<sup>2</sup> of latex.

concentration of Cu(II) in the reaction media. This is very different from our previous experience with DMA grafting where the PDI of the grafted polymer decreased and grafting density remained constant with addition of Cu(II) complex.<sup>23</sup> There are two possibilities for these differences in the behavior for DMA and NIPAM. One is that there are inherent differences in the properties or reactivity of the two monomers, resulting in the differences observed. The other is that the latexes used in the two series of experiments differed significantly in surface charge density, as this will determine the surface concentration of Cu(II) complex.<sup>23</sup> However, there is little difference in this parameter, and we found very similar DMA grafting characteristics with both latex (data not shown) so this is unlikely to be the explanation. We therefore believe the difference in the monomer is responsible for the difference in polymerization behavior observed.

Literature reports show that the nature of the interactions between Cu(II) complexes and radicals are important in producing controlled reactions, especially in aqueous solutions.<sup>53–55</sup> These interactions vary, depending on both monomer type and molecular weight,<sup>55</sup> producing broader molecular weight distributions and higher experimental molecular weights than theoretical  $M_n$  with increase in concentration of Cu(II) complex. For example, Matyjaszewski et al. showed that, in the case of AIBN-initiated styrene and methyl acrylate polymerization catalyzed by Cu(OTf)<sub>2</sub> and 4,4'-di-5-nonyl-2,2'-bipyridine, the effect of Cu(II) complex is only shown in styrene polymerization and not in the case of methyl acrylate.<sup>55</sup> It has also been reported that the Cu(II) effect is greater for high molecular weight polystyrene chains ( $M_n > 50\,000$ ), and the effect increases with molecular weight of chains.<sup>55</sup> Our results suggest that, although conversion and molecular weight decreased with concentration of Cu(II) as expected, interactions between PNIPAM macroradicals and Cu(II) complexes producing unwanted reactions may be the reason for the



Table 5. Characteristics of Block Copolymerization and Block Polymer Brush

sample	monomer	monomer concn (wt %)	$M_n$	$M_w/M_n$	$M_n$ (second block PDMA)	HT <sup>a</sup> first block (nm)	HT <sup>b</sup> second block (nm)
13 <sup>c</sup>	NIPAM <sup>e</sup>	6.1	211 000	1.18		265	
14 <sup>d</sup>	DMA <sup>f</sup>	17.00	525 000	1.35	314 000	265	429

<sup>a</sup> HT = hydrodynamic thickness. <sup>b</sup> HT of the second block is calculated as the one-half the difference between the hydrodynamic size of the PNIPAM grafted particles and PNIPAM-*b*-PDMA grafted particles. <sup>c</sup> Experimental conditions: 15 g of 3 wt % suspension of latex: HMTETA (0.23 mmol), CuCl (46  $\mu$ mol), CuCl<sub>2</sub> (88  $\mu$ mol), Cu powder (63  $\mu$ mol), NIPAM (7.7 mmol), methyl 2-chloropropionate (2  $\mu$ L), reaction temperature 22 °C. Surface initiator concentration =  $(1.56 \pm 0.05) \times 10^{-6}$  mol/m<sup>2</sup> of latex. <sup>d</sup> 3 g of 1.75 wt % suspension of PNIPAM grafted latex: HMTETA (62  $\mu$ mol), CuCl (13  $\mu$ mol), CuCl<sub>2</sub> (22  $\mu$ mol), Cu powder (16  $\mu$ mol), DMA (5 mmol), reaction temperature 22 °C. <sup>e</sup> *N*-Isopropylacrylamide. <sup>f</sup> *N,N*-Dimethylacrylamide.

increased PDI of PNIPAM chains with increase in the concentration of Cu(II). The effect is more pronounced in the present case than with other monomers which may be due to the higher molecular weight of the PNIPAM produced in this reactions.<sup>55</sup> This suggests that optimal reaction conditions may be unique for a particular monomer.

The hydrodynamic thicknesses of the brush systems are also given in Table 4. The HT decrease is due to a combination of molecular weight and chain density decrease as the Cu(II) is increased.

Addition of a small amount of soluble external initiator is known to increase the control of surface-initiated ATRP reactions in some cases.<sup>21,23</sup> We therefore varied the concentration of a hydrophobic initiator, methyl 2-chloropropionate, keeping other reaction conditions constant. The grafted latex was analyzed; characteristics of the grafted chains and properties of the brush layer are given in Table 4. Molecular weight and PDI of the grafted polymer decreases with increasing the concentration of external initiator. These are similar to the results seen with DMA when the surface initiator concentration was increased at constant monomer concentration.<sup>29</sup> The grafting density of the chains also decreased when external initiator was added. The hydrophobic external initiator used in our study would be expected to adsorb to the PS latex surface where the grafting reactions are taking place. Thus, addition of a small amount of external initiator is almost equivalent to increasing the surface concentration of initiator. Depending on the total surface initiator concentration that results, this could cause depletion of Cu(I)/ligand or monomer in the surface layer relative to the case in which no external initiator is present, thus changing the initiation and radical transfer processes that occur in the early stages of the reaction and reducing the number of chains grafted. The hydrodynamic thickness of the grafted layers is given in Table 4 and can be seen to decrease with decreasing molecular weight and graft density, as expected.

**Block Copolymerization.** These experiments were designed to demonstrate that the mechanism of the graft polymerization taking place in these experiments is ATRP. In ATRP reactions the chain ends of the grafted polymer chains are terminated with an active halogen atom. This end group can be used for further chain extension experiments with the same or a different monomer in the presence of catalyst. Table 5 gives the result of block copolymerization experiments from PNIPAM grafted latex particles. The molecular weight and hydrodynamic size of the PNIPAM-*b*-PDMA grafted particles increased considerably from the initial PNIPAM grafted particles. The PDI values for the polymers are low and show a slight increase from the PNIPAM first block. The  $dn/dc$  of the block copolymer (0.1525 mL/g) was calculated from the wt % composition value ob-

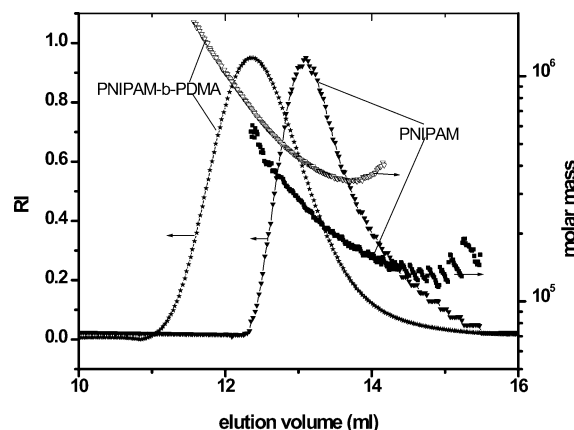
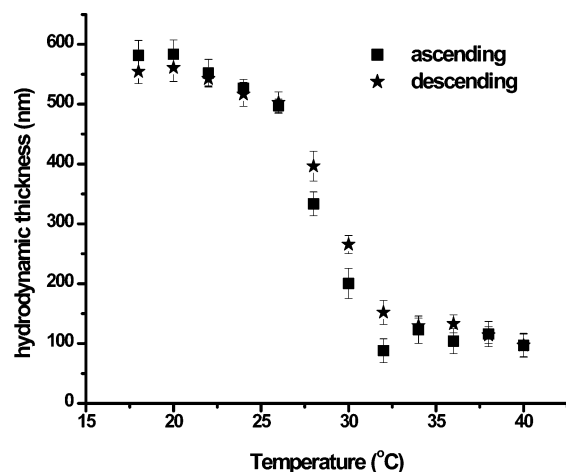


Figure 3. GPC chromatogram and molar mass vs elution of volume of PNIPAM first block and PNIPAM-*b*-PDMA block copolymer. Molar mass of the polymers was measured by multiangle light scattering detector DAWN EOS at room temperature (22 °C) in 0.1 N NaNO<sub>3</sub> solution.

tained from <sup>1</sup>H NMR of cleaved copolymer. Figure 3 shows the chromatogram of the block copolymer PNIPAM-*b*-PDMA with 211 000 PNIPAM as the first and 314 000 PDMA as the second block.

The molar mass vs elution volume for homo and block copolymer is also given in Figure 3. There is a large shift in elution volume for the copolymer peak in the RI chromatogram relative to that of the PNIPAM first block. The plots for molar mass for both polymers do not have any common points as shown in Figure 3 and are well separated. One would expect an overlapping region if some chains in the PNIPAM layer were not reinitiated to form PNIPAM-*b*-PDMA.<sup>56,57</sup> The increase in molecular weight with low polydispersity, increase in the hydrodynamic size of reinitiated PNIPAM grafted particles, and separation of PNIPAM and PNIPAM-*b*-PDMA molar mass vs elution volume curves (Figure 3) clearly demonstrate the high efficiency of the chain extension experiments. These results confirm that radical coupling or other chain end group modification are not the cause of termination of the polymer chains, unlike some ATRP grafting reactions of acrylamides in organic media.<sup>31–33</sup>

**Environmental Sensitivity of PNIPAM Brushes.** PNIPAM is known to be sensitive to a variety of environmental conditions such as temperature and salt concentration.<sup>34–36</sup> Homopolymers, hydrogels, and tethered chains of PNIPAM show a lower critical solution temperature (LCST) around 32 °C.<sup>36,58,59</sup> Below the LCST the polymer adopts a coiled structure, and above this temperature it collapses into a more globular form. In the case of a PNIPAM brush, one should be able to take advantage of its temperature or salt sensitivity to control the thickness of the grafted polymer layer, which could have a number of practical applications. Repre-



**Figure 4.** Dependence of hydrodynamic thickness (HT) of the PNIPAM brush ( $M_n = 796\,000$ ,  $M_w/M_n = 1.26$ , and grafting density =  $0.043$  chains/nm<sup>2</sup>) with temperature at pH = 7.1. The HT was measured by a temperature-controlled particle size analyzer with an equilibration time of 15 min for each temperature.

sentative data showing the temperature sensitivity of the grafted PNIPAM are given in Figure 4. The hydrodynamic thickness of the brush decreases with increasing temperature. Unlike homopolymers or hydrogels, however, the grafted PNIPAM layer does not show a sharp transition at 32 °C. Rather, the brush shows a smooth transition starting at 22 °C and continuing to 36 °C. These results are consistent with the reports in the literature on surface-grafted PNIPAM chains.<sup>41,59</sup>

Because of the high graft densities in these brushes, interchain interactions may be playing a role in the collapse of PNIPAM chains with decreasing solvent quality on increasing temperature. The coil-globule transition of grafted chains on the surface depends on solvent quality, interchain interactions, and the curvature of the surface on which the polymer chains are grafted, i.e., planar, cylindrical, or spherical.<sup>60</sup> It has been predicted for spherical brushes that the transition is second order, and the collapse of the grafted layer starts from the outer, dilute portion of the layer, since the density of chains decreases monotonically with distance away from the surface.<sup>60</sup> The chain density of the sample examined here decreases almost 9 times from the outer edge of the brush (sample 12, Table 3) to the latex surface. Interchain interaction in the grafted polymer layer makes the collapse transition weaker than in an isolated three-dimensional chain,<sup>60</sup> since interchain contacts can reduce solvent-monomer interactions without inducing chain contraction. Thus, one expects a broader range in the hydrodynamic thickness change with a decrease in solvent quality for brushes. Currently we are investigating the effect of grafting density of the chains on temperature-induced collapse of grafted PNIPAM chains to provide more insight into the role of chain-chain interactions on the conformation of grafted PNIPAM chains.

The cooling curve, Figure 4, shows that hydration and expansion of the collapsed brush does not follow the same path as the collapse on heating, utilizing the time course applied here (15 min equilibration per temperature). The hydrodynamic size of the grafted latex essentially regains its original size upon cooling from high temperature to low temperature, the hydration again occurring over a broad temperature range as the

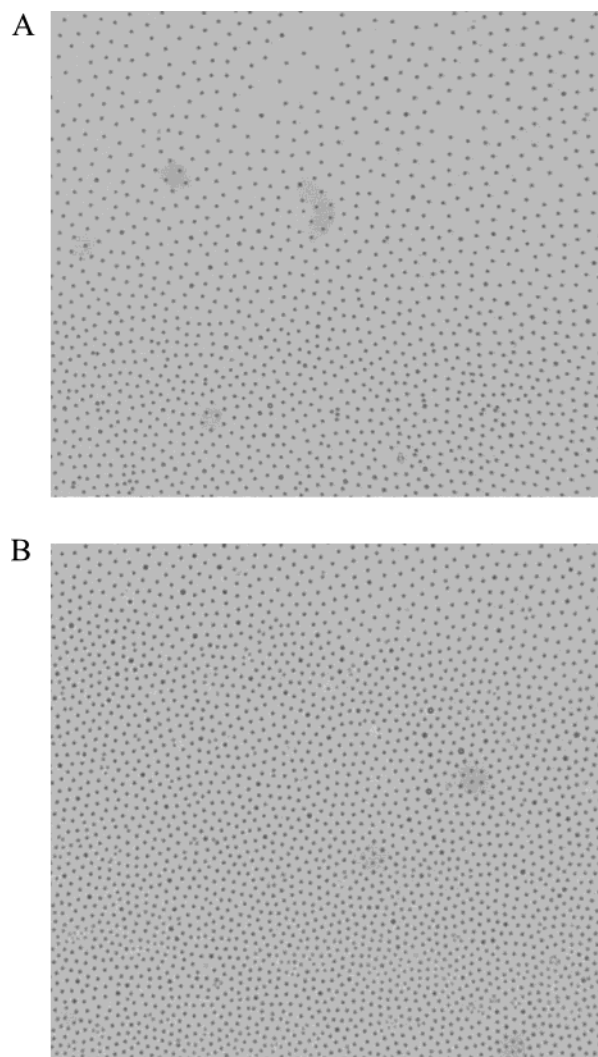


**Figure 5.** Optical micrographs of PNIPAM brush in water (same sample as for Figure 4) above and below LCST. (A) 20 °C and (B) 40 °C.

coil expands. Similar hysteresis behavior has been reported for grafted as well as PNIPAM solutions by other groups.<sup>41,58</sup> Repeated heating and cooling cycles showed the fully collapsed and hydrated dimensions were retained.

To examine whether the grafted latex aggregated on heating, we observed their aqueous suspensions by optical microscopy at temperatures below and above the LCST, i.e., 20 and 40 °C. The optical micrographs of the latex settled on a glass slide (Figure 5) show that the PNIPAM grafted latex remains as individual particles even after the collapse of the chains on the surface. The variations in particle separation in different areas of the images at both temperatures are likely due to variations in particle concentration produced during flow of the suspension that occurs while placing a coverslip on the drop of suspension. Variation in the degree to which the particles interact with the two surfaces and edge effects can produce such variation. The main observation is that no large inhomogeneities associated with three-dimensional aggregates with accompanying large particle-free areas are observed.

In a final set of experiments, the coil-globule transition of grafted PNIPAM was studied with addition of salts in solution at pH 7.4. PNIPAM is sensitive to NaCl and Na<sub>2</sub>SO<sub>4</sub>, and these salts induce phase transitions



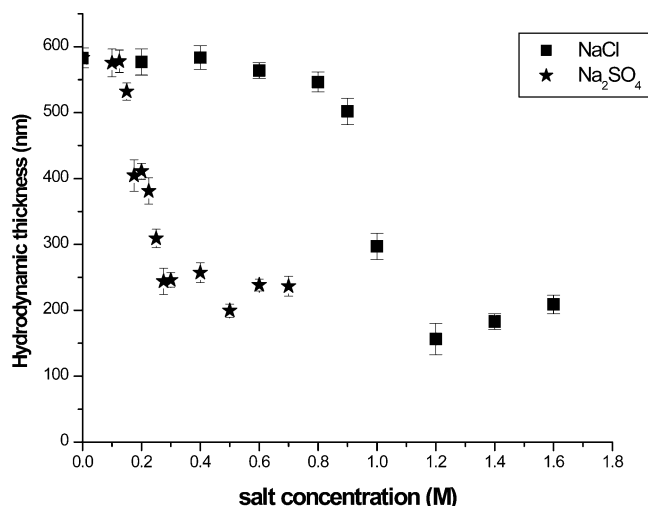


**Figure 6.** Dependence of hydrodynamic thickness of the PNIPAM brush ( $M_n = 796\,000$ ,  $M_w/M_n = 1.28$ , and grafting density =  $0.043$  chains/nm<sup>2</sup>) with salt concentration at pH 7.4. The HT was measured at 20 °C by a temperature-controlled particle size analyzer.

at different concentrations in solution. In our experiments we varied the concentration of NaCl from 0 to 1.6 M and 0 to 0.7 M for Na<sub>2</sub>SO<sub>4</sub> and measured the hydrodynamic size of the particles as a function of concentration for each salt. The measured hydrodynamic thicknesses of the particles are given in Figure 6. The HT decreases with increasing salt concentration in both cases. Na<sub>2</sub>SO<sub>4</sub> induces a transition around 0.2 M and NaCl at ~1.0 M for PNIPAM grafted particles; this is consistent with earlier reports.<sup>36</sup>

The collapsed brushes formed by three different stimulants have different values of HT as seen in Figures 4 and 6. By comparing Figure 4 and Figure 6, it is seen that the temperature has a larger effect on the collapse of PNIPAM brushes than salts. The effect of different stimulants on the collapse of brush used in this study therefore decreases in the order temperature > NaCl ~ Na<sub>2</sub>SO<sub>4</sub>.

## Conclusions

We have successfully synthesized narrowly dispersed PNIPAM chains on functionalized latex particles by surface-initiated aqueous ATRP reactions. The grafted polymer brushes were characterized by determining the molecular weight, grafting density, and height of the grafted polymer layers on the surface. The molecular weights of the polymer chains were controlled by adjusting reaction parameters such as monomer concentration, concentration of Cu(II) complex, and addition of external initiator. Polymers with a wide range molecular weights from ~50 000 to 800 000 were obtained. By an efficient block copolymerization, we demonstrated that the grafting reactions are taking place by the ATRP mechanism. The grafted PNIPAM layers are in the true brush regime as shown by the large hydrodynamic thickness and small  $D/R_g$  values. The hydrodynamic thickness of the brushes ranges from ~100 to 600 nm. The thickness of these PNIPAM layers varies as  $(DP)^{0.66}$  at constant grafting density. The PNIPAM brush thicknesses were shown to be sensitive to temperature and salt concentration, but a broader transition temperature range is observed for PNIPAM brush collapse compared to the sharp transition for linear chains in solution. The height of the collapsed brush depends on the agent used for inducing the phase transition.

**Acknowledgment.** We thank the Canadian Institutes of Health Research, National Science and Engineering Council Canada, the Canada Foundation for Innovation, and Canadian Blood Services for financial support.

**Supporting Information Available:** Experimental procedures and results of the surface adsorption of DMA and NIPAM on shell latex. This material is available free of charge via the Internet at <http://pubs.acs.org>.

## References and Notes

- (1) Lahann, J.; Mitragotri, S.; Tran, T.; Kaido, H.; Sundram, J.; Choi, I. S.; Hoffer, S.; Somarjai, G. A.; Langer, R. *Science* **2003**, *299*, 371–374.
- (2) Okano, T.; Kikuchi, A.; Sakurai, Y.; Takei, Y.; Ogata, N. *J. Controlled Release* **1995**, *36*, 125–133.
- (3) Chaudhury, M. K.; Whitsides, G. M. *Science* **1992**, *256*, 1539–1541.
- (4) Pan, V. Y.; Wesley, R. A.; Lyginbuhl, R.; Denton, D. D.; Ratner, B. D. *Biomacromolecules* **2001**, *2*, 32–36.
- (5) Russell, T. P. *Science* **2002**, *297*, 964–967.
- (6) Nagasaki, Y.; Kataoka, K. *Trends Polym. Sci.* **1996**, *4*, 59–64.
- (7) Jones, D. M.; Smith, R. R.; Huck, W. T. S.; Alexander, C. *Adv. Mater.* **2002**, *14*, 1130–1134.
- (8) Kidoaki, S.; Ohya, S.; Nakayama, Y.; Matsuda, T. *Langmuir* **2001**, *17*, 2402–2407.
- (9) Kikuchi, A.; Okano, T. *Prog. Polym. Sci.* **2002**, *27*, 1165–1193.
- (10) Kanazawa, H.; Yamamoto, K.; Matsushima, Y.; Takai, N.; Kikuchi, A.; Sakurai, Y.; Okano, T. *Anal. Chem.* **1996**, *68*, 100–105.
- (11) Hester, J. F.; Olugebefola, S. C.; Mayes, A. M. *J. Membr. Sci.* **2002**, *208*, 375–388.
- (12) Ito, Y.; Park, Y. S.; Imanishi, Y. *J. Am. Chem. Soc.* **1997**, *119*, 2739–2740.
- (13) Cunliffe, D.; de Alarcon, C.; Peters, V.; Smith, J. R.; Alexander, C. *Langmuir* **2003**, *19*, 2888–2899.
- (14) Okano, T.; Yamada, N.; Oukara, M.; Sakai, H.; Sakurai, Y. *Biomaterials* **1995**, *16*, 297–203.
- (15) Zhao, B.; Brittain, W. J. *Prog. Polym. Sci.* **2000**, *25*, 677–710.
- (16) Milner, S. T. *Science* **1991**, *251*, 905–914.
- (17) Jordan, R.; Ulman, A.; Kang, J. F.; Rafailovich, M. H.; Sokolov, J. *J. Am. Chem. Soc.* **1999**, *121*, 1016–1022.
- (18) Jordan, R.; Ulman, A. *J. Am. Chem. Soc.* **1998**, *120*, 243–247.
- (19) von Werne, T.; Patten, T. E. *J. Am. Chem. Soc.* **2001**, *123*, 7497–7505.
- (20) Kim, J. B.; Bruening, M. L.; Baker, G. L. *J. Am. Chem. Soc.* **2000**, *122*, 7616–7617.
- (21) Matyjaszewski, K.; Miller, P. J.; Shukla, N.; Immaraporn, B.; Gelman, A.; Luokala, B. B.; Siclován, T. M.; Kickelbick, G.; Vallant, T.; Hoffmann, H.; Pakula, T. *Macromolecules* **1999**, *32*, 8716–8724.
- (22) Ejaz, M.; Yamamoto, S.; Ohno, K.; Tsujii, Y.; Fukuda, T. *Macromolecules* **1998**, *31*, 5934–5936.
- (23) Jayachandran, K. N.; Takacs-Cox, A.; Brooks, D. E. *Macromolecules* **2002**, *35*, 4247–4257.
- (24) Sedjo, R. A.; Mirov, B. K.; Brittain, W. J. *Macromolecules* **2000**, *33*, 1492–1493.
- (25) Wang, X. S.; Armes, S. P. *Macromolecules* **2000**, *33*, 6640–6647.
- (26) Perruchot, C.; Khan, M. A.; Kamitsi, A.; Armes, S. P.; von Werne, T.; Patten, T. E. *Langmuir* **2001**, *17*, 4479–4481.
- (27) Guerrini, M. M.; Charleux, B.; Vairon, J. P. *Macromol. Rapid Commun.* **2000**, *21*, 669–674.
- (28) Jones, D. M.; Huck, W. T. S. *Adv. Mater.* **2001**, *13*, 1256–1259.
- (29) Kizhakkedathu, J. N.; Brooks, D. E. *Macromolecules* **2003**, *36*, 591–598.
- (30) Kizhakkedathu, J. N.; Goodman, D.; Brooks, D. E. *Advances in Controlled/Living Polymerization*, Matyjaszewski, K., Ed.; ACS Symp. Ser. **2003**, *854*, 316–330.
- (31) Xiao, D. Q.; Wirth, M. J. *Macromolecules* **2002**, *35*, 2919–2925.
- (32) Teodorescu, M.; Matyjaszewski, K. *Macromolecules* **1999**, *32*, 4826–4831.
- (33) Rademacher, J. T.; Baum, R.; Pallack, M. E.; Brittain, W. J.; Simonsick, W. J. *Macromolecules* **2000**, *33*, 284–288.

- (34) Heskins, M.; Guillet, J. E.; James, E. *J. Macromol. Sci., Chem. A2* **1968**, 1441–1455.
- (35) Gao, J.; Wu, C. *Macromolecules* **1997**, 30, 6873–6876.
- (36) Park, T. G.; Hoffman, A. S. *Macromolecules* **1993**, 26, 5045–5048.
- (37) Ding, X.; Sun, Z.; Zhang, W.; Peng, Y.; Wan, G.; Jiang, Y. *J. Appl. Polym. Sci.* **2000**, 77, 2915–2920.
- (38) Collier, T. O.; Anderson, J. M.; Kikuchi, A.; Okano, T. *J. Biomed. Mater. Res.* **2002**, 59, 136–143.
- (39) Stayton, P. S.; Shimoboji, T.; Long, C.; Chilkoti, A.; Chen, G. H.; Harris, J. M.; Hoffman, A. S. *Nature (London)* **1995**, 378, 472–474.
- (40) Wang, G. Q.; Kuroda, K.; Enoki, T.; Grosberg, A.; Masamune, S.; Oya, T.; Takeoka, Y.; Tanaka, T. *Proc. Natl. Acad. Sci. U.S.A.* **2000**, 97, 9861–9864.
- (41) Balamurugan, S.; Mendez, S.; Balamurugan, S. S.; O'Brien, M. J.; Lopez, G. P. *Langmuir* **2003**, 19, 2545–2549.
- (42) Vanderhoff, J. W.; Van den Hul, H. J.; Tausk, R. J. M.; Overbeek, T. T. G. In *Clean Surfaces*; Goldfinger, G., Ed.; Marcel Dekker: New York, 1970; pp 15–44.
- (43) Hirtcu, D.; Muller, W.; Brooks, D. E. *Macromolecules* **1999**, 32, 565–573.
- (44) Kizhakkedathu, J. N.; Norris-jones, R.; Brooks, D. E. Manuscript in preparation.
- (45) Xia, J. H.; Matyjaszewski, K. *Macromolecules* **1997**, 30, 7697–7700.
- (46) Zhu, P. W.; Napper, D. H. *J. Colloid Interface Sci.* **1994**, 164, 489–494.
- (47) Brandrup, J.; Immergut, E. H., Eds. *Polymer Handbook*; John Wiley & Sons: New York, 1989.
- (48) Dan, N.; Tirrell, M. *Macromolecules* **1992**, 25, 2890–2895.
- (49) de Gennes, P. G. *J. Phys. (Paris)* **1976**, 37, 1445–1452; *Macromolecules* **1980**, 13, 1069–1075.
- (50) Alexander, S. *J. Phys. (Paris)* **1977**, 38, 983–987.
- (51) Wijmans, C. M.; Zhulina, E. B. *Macromolecules* **1993**, 26, 7214–7224.
- (52) Matyjaszewski, K.; Patten, T. E.; Xia, J. *J. Am. Chem. Soc.* **1997**, 119, 674–680.
- (53) Kochi, J. K. *Acc. Chem. Res.* **1974**, 7, 351–360.
- (54) Navon, N.; Golub, G.; Cohen, H.; Meyerstein, D. *Organometallics* **1995**, 14, 5670–5676.
- (55) Matyjaszewski, K.; Woodworth, B. E. *Macromolecules* **1998**, 31, 4718–4723.
- (56) DAWN, ATSTRA for Windows User's Guide, version 4.70; Wyatt Technology Corp., Santa Barbara, CA, 1998.
- (57) Our experimental verification by analyzing narrowly dispersed PEG and protein samples of different molecular weight on the DAWN-EOS multiangle detector also support this argument. The peak width in the chromatogram is due to the column broadening and the molar mass–elution volume plot is typically a flat line (parallel to elution volume axis) for monodispersed sample. Two samples with different molecular weights never had common points in the molar mass–elution volume graph.
- (58) Hu, T.; You, Y.; Pan, C.; Wu, C. *J. Phys. Chem. B* **2002**, 106, 6659–6662.
- (59) Zhu, P. W.; Napper, D. H. *J. Phys. Chem. B* **1997**, 101, 3155–3160.
- (60) Zhulina, E. B.; Borisov, O. C.; Pryamitsyn, V. A.; Brishtein, T. M. *Macromolecules* **1991**, 24, 140–149.

MA034934U